SAND2012-0085C

LASER-DIAGNOSTIC MAPPING OF TEMPERATURE AND SOOT STATISTICS IN A SOOTING TURBULENT POOL FIRE

Sean P. Kearney, Thomas W. Grasser, Daniel Scoglietti, Dann Jernigan, and Thomas K. Blanchat

Engineering Sciences Center
Sandia National Laboratories
Albuquerque, NM 87185 USA

Submitted to the 34th Symposium (International) on Combustion
Warsaw, Poland
July 29-August 3, 2012

Corresponding Author: Sean P. Kearney
Sandia National Laboratories
P.O. Box 5800; Mail Stop 0826
Albuquerque, NM 87185 USA
Voice: +1-505-844-6669
Email: spkearn@sandia.gov

Colloquium: Fire Research

Alternate Colloquium: Diagnostics

Total Length: XXXX words determined using Method 1

Word Equivalent Lengths:

Main Text:
References:
Figure 1:
Figure 2:
Figure 3:
Figure 4:
Figure 5:
Figure 6:

Total Words Equivalent for Figures =
Total Figures = 6, 2 color

Abstract

We present spatial profiles of temperature and soot-volume-fraction statistics from a sooting 2-m base diameter turbulent pool fire. Dual-pump coherent anti-Stokes Raman scattering (CARS) and laser-induced incandescence (LII) are utilized to obtain profiles of temperature and soot probability density functions (pdf) at three vertical heights above the surface of the methanol/toluene fuel pool. The experiments are conducted in the unique Sandia FLAME facility, which has recently been modified to allow for vertical translation of the optical systems and horizontal translation of the liquid fuel burner. Results are presented both in the fuel vapor-dome region at ¼ base diameter and in the actively burning region at ½ and ¾ diameters above the fuel surface. The evolution of the soot and temperature pdfs is discussed and profiles of the temperature and soot mean and rms statistics are provided. These new validation-quality results provide profiles of the key soot radiative-emission parameters at volumetric resolution comparable to flame length scales and can be used for detailed development and validation of fire fluid dynamics models.

Keywords: Fire research; pool fire; soot; laser diagnostics

1. Introduction

Fire is a leading threat to the security of transportation systems, critical infrastructure, and human life in a wide range of both civilian and military accident scenarios. Improved computational tools for high-consequence fire risk assessment are increasingly relying upon more solid physical underpinnings for truly predictive simulation of fire phenomena. Fire fluid dynamics codes must capture complex, multi-physics effects, encompassing buoyancy driven turbulent mixing; chemical reaction; and the net thermal radiative transport that is a product of the reacting flow—all in a three-dimensional system that is several meters or more in size. These large-scale simulations are costly, and detailed experiments are extraordinarily valuable for both development of appropriate subgrid and engineering models that make the simulations more tractable, and for validation of the simulation output for flames of realistic size.

Both the nature and the quality of the experimental data that can be extracted from a canonical meter-scale wind-free fire plume has been dramatically improved by adapting the laser-diagnostic tools that have revolutionized laboratory combustion research [1]to larger scale systems. Many critical aspects of the reacting flow problem can now be probed. Buoyancy driven turbulence statistics and flow physics have been investigated for 1-m diameter methane and hydrogen fires using particle-image velocimetry (PIV) [2], and the turbulent mixing in a 1-m base buoyant helium plume has been obtained using combined PIV and planar laser-induced fluorescence [3]. Fire thermal radiative emission is the key element of risk, and optical diagnostics have now been utilized to monitor both the net path-integrated radiation (the “effect” of primary importance), as well as the spatially resolved soot emitter and temperature fields (the “cause”) which generate the global radiation field. Emission spectroscopy has revealed path-integrated thermal radiation spectra at kHz rates to provide quantitative insight into the net fire radiative output [4, 5]. Local emission/absorption measurements [6] and tunable-diode-laser

absorption spectroscopy [7] have revealed soot (emitter) concentration and temperature at spatial resolutions of a few cm in jet-fuel fires of 1-5 meters in base size.

These earlier measurements, while revealing, are still limited in their spatial resolution, which at several cm still averages over several emitting flame structures. We have recently described improved instrumentation for temperature and soot measurements in large fires at volumetric spatial resolutions as fine as 10^{-4} cm^3 for temperature and 10^{-5} cm^3 for soot by utilizing dual-pump coherent anti-Stokes Raman scattering (CARS) thermometry [8, 9] and laser-induced incandescence (LII) [10]. This work was facilitated by the unique Sandia Fire Laboratory for Accreditation of Models and Experiments (FLAME) facility [11], which allows for controlled meter-scale burns with integrated laser diagnostics. Our earlier work demonstrated capability, but provided limited data at only a single measurement point and for a restricted number of laser shots and fire realizations that was too small for meaningful statistics to be generated. We have now applied these laser-diagnostic tools in a large data campaign in which the temperature/soot statistics were mapped across a 2-m base diamter fire plume at multiple spatial locations with large ensembles of single-laser-shot measurements gathered over multiple fire experiments to gather more meaningful statistical results. The FLAME facility was significantly modified in this process, adding new hardware for practical vertical translation of the laser measurement volume and horizontal translation of the liquid fuel burner. We describe the modifications to our already unique fire research facility, and present the results of our recent data campaign here.

2. FLAME Facility

The design and construction of FLAME is described in significant detail by Blanchat *et al*. [11]. Briefly, a 2-m fuel pan is located at the center of an 18.3-m diameter × 12.2-m high main test bay level, whose water-cooled walls provide a well-controlled ambient temperature far-field condition. Combustion air is provided through a well-balanced air ring at the periphery of the FLAME basement

level and entrained through steel-grated flooring at the perimeter of the main test-bay level. A smooth ground plane is provided by a 12-m outer diameter steel skirt that surrounds the liquid fuel pan. Fuel is maintained at a constant level just below the fuel-pan lip throughout the experiment by pumping fuel into the bottom of the pan at a rate adjusted by monitoring the fuel surface liquid level with a rake of fine-wire thermocouples that spiked in temperature when the junctions penetrated the pool surface. A research fuel blend of 10% toluene by volume in a balance of methanol is used in our experiments. Addition of heavily sooting toluene to clean-burning methanol allows us to achieve a balance between fuel sooting propensity, fire optical thickness, and heat transfer to optical elements located in proximity to the fire plume. The flame height of the resulting 2-m base diameter fire plume is nominally 2 m, based on time-exposed imaging of visible soot emission. The facility provides a canonical “wind-free” fire plume that stands essentially straight up without listing from one side to another during the CARS/LII experiments.

Significant new capabilities were added to FLAME to provide us with the ability to raster the laser measurement volume throughout the fire plume. A digital drawing of the FLAME test bay level with the fuel-pan, optical hardware enclosures, and positioning platforms is shown in Figure 1. Three water-cooled enclosures housed the CARS beam-crossing lens, CARS collection optics, and the LII imaging optics directly adjacent to the fire plume. The optical enclosures are mounted to three individually adjustable precision lifting platforms, allowing us to position the laser measurement volume anywhere from 0.5 to 1.8 m above the fuel-pool surface. The fuel pan was additionally mounted to a rail system and could be horizontally translated a distance of 1 m (1 pan radius) using a remotely actuated motor. All drive motors, pulleys and control systems are located at the FLAME basement level to shield this equipment from heat. Thermal expansion of lifting platform supports exposed to fire radiative fluxes is minimized with judicious choice of materials and by insulating the supports with 50-mm thick

"kaowool" jackets wrapped in a reflecting stainless-steel foil. This arrangement allows us to maintain sufficient CARS signal for 1-2 hours of burn time, over which the fuel pan is horizontally scanned with the optics maintained at constant height. CARS and LII data are obtained on a single-laser-shot basis with several thousand laser shots acquired at each location before moving the fuel pan. Data are acquired in the hottest regions, near the center of the fire, first so that degradation of the CARS signal strength over the course of an experiment is balanced by increased CARS signals in the colder gas that is encountered as the CARS measurement volume is scanned radially outward. Laser-diagnostic data has been acquired at heights of 0.5, 1.0 and 1.5 m above the liquid fuel surface. Multiple burns were conducted at each measurement height to both increase the size of the data ensemble and to capture any effects of day-to-day variation of the FLAME test bay conditions. Nominally 20,000 laser shots were acquired at each point near the center of the fire plume, with a lesser number (2,000 to 10,000) acquired at outer locations where less soot and high temperature fluctuations occurred.

3. Laser-Diagnostic Instrumentation and Data Analysis

Design of our dual-pump CARS [12] and LII [13] instrumentation is described in detail in refs. [8-10], and is only briefly summarized here. For CARS, an injection-seeded, frequency-doubled Nd:YAG laser pumps a narrowband, tunable commercial dye laser and a home-built broadband dye laser. Two frequency-narrow CARS pump beams at 532 and 554 nm, and a broadband Stokes beam centered at 607 nm are arranged in a folded phase-matching configuration [14] and ported through a BK-7 window into the FLAME test bay, where they are mirror coupled by a height-adjustable, remote-controlled periscope to a 1000-mm focal length CARS beam crossing lens in a water-cooled enclosure adjacent to the pool fire. CARS signal radiation is generated near 491 nm, in a spectral region where interference from laser-generated C_2 emission [15] and C_2 Raman [16] interferences is minimized. A second water-cooled

enclosure is located opposite the beam-crossing lens, where an additional 1000-mm focal length lens collimates the CARS signal, and dichroic mirrors separate the CARS beam from the pump and Stokes radiation before the signal is launched into a 100-μm-core multimode fiber, which transmits the CARS signal for detection by a 0.75-m spectrometer and back-illuminated CCD located in the main laser lab. For LII, a second *Q*-switched Nd:YAG laser (unseeded) provides an 8-ns 1064-nm beam, which is formed into a nominally 5-mm high × 1-mm thick sheet coincident with the CARS measurement volume by using a combination of sheet-forming cylindrical and spherical elements located in the remote laser lab in conjunction with the CARS beam-crossing lens. LII is generated in the plateau-level regime [13, 17] with a beam fluence near 2 J/cm^2 and imaged using a water-cooled probe described in detail in ref. [10]. This probe contains optics to relay image the LII laser sheet volume at unit magnification onto the face of a 1-million-element coherent fiber imaging bundle that transmits the signal to a gated intensified CCD detector at the FLAME basement level. All laser beams are delivered to the measurement volume through a steel light pipe that tapers to a 25-mm diameter approximately 100 mm from the measurement volume. A second, identical steel pipe is used to transmit the CARS signal to the collection optics, resulting in a 200-mm beam path through the beam-steering, optically absorbing pool fire, as shown in Figure 1.

Single-laser-shot data are recorded at 10 Hz, with the LII laser pulse arriving 10 μs before the CARS pump and Stokes beams, so that the LII measurements are not contaminated by significant laser vaporization of soot by the intense CARS beams. CARS temperatures are deduced by performing theoretical fits to the N_2 *Q*-branch portion of the CARS spectrum, shown in Figure 2a, using the Sandia CARSFT code [18]. Temperature, relative nonresonant-background contribution, and parameters accounting for horizontal and vertical shifts in the spectra are varied in CARSFT. Nitrogen self line broadening was employed due to lack of knowledge of the shot-to-shot collision partner distribution.

Further details on CARS spectral fitting can be found in refs. [8, 9]. The precision of the single-shot CARS temperatures was estimated at ±3.5-5% with an accuracy of 2-3% based on measurements in tube-furnace-heated air at 300-1400 K and a near-adiabatic methane-air flame from 1900-2200 K. The LII images are calibrated for soot volume fraction using a Santoro-style C_2H_4/air laminar diffusion flame [19] that is brought into the FLAME test bay at the beginning of each testing day. A portion of the 1064-nm LII beam is tightly apertured and used to perform a light-extinction measurement at a reference height of 35 mm above the fuel-nozzle exit. LII images are recorded at the reference location using the full, unapertured, laser sheet and a calibration factor between LII detector counts and soot volume fraction is obtained by comparing the integrated LII signal along the extinction beam path to the measured light attenuation, as described in [10]. Light-extinction calibration was time consuming and was not performed daily, but LII imaging in the Santoro flame was checked each day to monitor any drifts in the LII system response. Peak LII counts in the Santoro reference flame varied by no more than ±20% over the course of the data campaign presented here.

The volumetric spatial resolution of the CARS measurements is 10^{-4} cm^3, based on a ~100-μm nominal beam focus and a rather long ~8-10 mm beam-overlap region. Fitting of the CARS spectra provides an enthalpy-pooled average temperature within the volume, which is subject to bias errors due to spatial-averaging or "density-weighting" effects [20] if significant gradients exist along the beam-overlap direction. We estimate these effects to be minimal, based on Rayleigh-scattering imaging of thermal gradients along the CARS measurement volume at the center of a methanol pool fire whose turbulence properties should be similar to the 90% methanol fuel used here, as explained in ref. [9]. The LII measurement volume is 10^{-5} cm^3, based on a 1-mm-thick laser sheet and a 100-μm resolution for the LII imaging optics. The LII signal represents a linearly weighted soot-volume-fraction measurement in this volume.

4. Results and Discussion

A shot-averaged CARS spectrum recorded with the measurement volume at a height of y = 0.5 m above the fuel surface at the center of the fuel pan (r = 0) is shown in Figure 2. This averaged spectrum shows contributions from the N_2 Q branch as well as H_2 S-branch rotational lines. The spectrum also exhibits significant nonresonant background from unburned hydrocarbons, as revealed by the broad, featureless background and modulation dip in the N_2 spectrum as well as significant contributions from laser-generated and naturally occurring C_2. These background contributions arise from the location of the CARS measurement volume within the "vapor dome" region [21] of the fire plume, where a significant amount of unburned pyrolized hydrocarbons are present. Significant unburned hycrocarbon was additionally confirmed infrared emission spectra along horizontal paths at y = 0.5 m, which revealed significant absorption in the C-H stretch region near 3.3 μm. We highlight this spectrum because measurements in this fuel rich region are challenging with many laser-diagnostic approaches. Representative single-laser-shot CARS spectra in the N_2-containing region only are shown in Figure 2b-d. Both measured spectra and the corresponding theoretical fits are shown in each of the three spectra. These spectra were recorded during the same burn, and at the same spatial location as the shot-averaged spectrum in Figure 2a and illustrate our ability to fit the data for reliable temperature measurements in this challenging fuel-rich region of the fire plume. The spectrum in Figure 2b represents a fit to low-N_2-content gases with significant nonresonant background, while the spectra in Figure 2c,d illustrate the nature our CARS spectra in hot gases at T = 1876 K and at a much colder temperature T = 960 K.

Three representative LII images recorded at the same spatial location as the CARS spectra in Figure 2 are shown in Figure 3. These images reveal a two-dimensional slice through complex three-dimensional soot structures with a 1-mm averaging depth in the out-of-plane direction. The uppermost image in Figure 3 shows layers imaged along their edges, revealed as thin structures of a few hundred

microns in layer thickness. The lower two images in Figure 3 are examples of soot sheets with their elongated directions largely within the plane of the LII laser sheet. In all cases, there is a significant amount of the image in which little or no soot appears with soot containing layers exhibiting a volume fraction, f_v, of order several hundred ppb (0.1s of ppm). This highly intermittent spatial structure was typical of the LII data recorded at all regions of the fire plume. Very few ppm-level fluctuations were observed with the 10% toluene-in-methanol research fuel blend used here.

Radial profiles of mean and rms fluctuating temperature and soot f_v for all three heights above the burner surface are shown in Figure 4, where smooth curves are faired through the more quantitative data points. Each profile is the result of a compilation of similar profiles obtained for different burns conducted on different days over a period of approximately 10 weeks. The error bars on the plots represent the maximum deviation of the single-burn profiles at a given measurement point and provide an estimate of any systematic errors arising from changes in facility conditions over time. The mean temperature profiles all peak at the radial center of the plume near T = 1400 K, and exhibit peak rms fluctuations near 400 K, at all three heights above the liquid burner. The peak in the rms temperature fluctuation moves inward with increasing height, from r = 30 cm at the near-surface location of y = 0.5 m, to r = 20 and 15 cm at y = 1.0 and 1.5 m, respectively. This behavior is consistent with the "neck down" of the fire plume with collapse of the vapor dome and movement of the peak mixing regions inward with increasing height above the fuel surface. The soot profiles shown in Figure 4 are markedly different than the temperature profiles. At a height of y = 0.5 m, the peak mean soot concentration appears off the centerline near r = 15 cm with the peak fluctuating soot levels occurring at the same location. The peak mean soot concentration decays with increasing height, from 6.5 ppb at y = 0.5 m to 5 ppb at y = 1.5 m. All profiles of temperature and soot statistics are quite similar for y = 1.0 and 1.5 m,

suggesting relatively minor changes in the structure of the fire plume once the vapor dome collapses above y = 0.5 m.

Probability density functions (pdf) of the temperature fluctuations at all locations were generated by binning all the single-shot CARS data into 50-K wide intervals and constructing histograms, with the results plotted in Figure 5. In all cases, the data have been normalized by the total area under each histogram so that the results represent true estimates of probabilities. At all three heights, the evolution of the pdf with increasing distance from the plume center is qualitatively similar. At the center of the plume the hottest gases are encountered with minimal mixing of low-temperature gases at the plume centerline; the pdf shapes are nominally Gaussian with a weak high-temperature skew at y = 0.5 m and a stronger low-temperature skew at y = 1.0 and 1.5 m, where width of the plume is less and the likelihood of low temperature gases reaching the centerline increases. The temperature pdfs then become nearly uniform at intermediate distances, ranging from r = 20 cm low in the plume to r = 10 cm at y = 1.5 m before obtaining a shape with significant high-temperature skewness at the outer regions of the plume where strong large-scale puffing motions [3] result in strongly intermittent high-temperature fluctuations on top of an increasingly low-temperature baseline.

Probability density functions of the LII-determined soot volume fractions for all measurement locations are presented in Figure 6. The pdfs were constructed by binning the LII signal from each pixel within a 2.35-mm high × 8.7-mm wide cropped region for all images within the ensemble. The bin width was 100 detector counts, corresponding to a soot volume fraction of 1.3 ppb, corresponding to 656 bins over the 853 ppb dynamic range of the LII instrument. The results represent an estimate of the pdf of the average soot loading in a 0.1 × 0.1 × 1 mm volume. At all heights above the liquid-fuel surface, the data exhibit a nearly logarithmic decay at locations closest to the center of the fire plume, where the average soot volume fractions are highest. The type of lognormal or “clipped” pdf signature is indicative of a

highly intermittent soot signal with a most likely value near zero and very large, positive fluctuations. Much different pdf shapes have been reported for meter-scale fires with real JP-8 transportation fuel. Murphy and Shaddix [7] and Gritzo *et al*. [6] present *in situ* emission/absorption soot f_v data from a 1-m and 5-m JP-8 fires, repectively; their soot-volume-fraction pdfs near the center of the plume are much closer to a normal or bi-modal distribution in shape. Some instances of clipped pdf structure are observed in [7] at locations high above the fuel surface, where increased mixing of cold, soot-free gas likely diluted the soot stream. Similar clipped soot pdfs have been reported by Henriksen *et al.* [22], who performed LII measurements in a 15-cm diameter JP-8 pool fire, and by Xin and Gore [23] who report LII data in buoyant 7.1-cm methane and ethylene flames. The small scale of these laboratory flames is likely the source of the discrepancy from the larger JP-8 fire results. Our fire plume is similar in size to the large JP-8 fires, but the significantly decreased sooting propensity of our research fuel blend relative to JP-8 likely alters the soot statistics in this case.

5. Summary and Conclusion

We have presented the results of a recent data campaign in which high-fidelity laser diagnostics have been used to obtain spatially resolved maps of temperature and soot statistics in a buoyant, liquid-fueled pool fire of meaningful meter-scale size. The experiments were performed in a 2-m base diameter fire plume with a 10% toluene/90% methanol research fuel blend selected to facilitate the use of laser diagnostics. Dual-pump CARS and LII were used to obtain single-laser-shot temperatures and soot-volume-fraction data with a volumetric spatial resolution of 10^{-4} and 10^{-5} cm^3, respectively. Extensive ensembles of single-laser-shot data acquired over many different pool-fire experiments allowed us to construct radial profiles of mean and rms fluctuating quantities and probability distributions at heights of 0.5, 1.0 and 1.5 m above the liquid fuel surface. Evolution of the temperature pdf structures reveals a

gradual transition from a hot-gas region at the center of the fire plume, with limited mixing with outside air, to an intermediate region with uniform pdf structure, and finally to a highly intermittent region with clipped or lognormal pdf structure. Soot pdf structure is nearly lognormal throughout the plume, in agreement with LII measurements performed in smaller laboratory scale buoyant flame systems, but in contrast to heavily sooting meter-scale fire experiments performed with real JP-8 transportation fuel. We surmise that the low-sooting toluene/methanol research blended fuel used here is the primary reason for these differences. These data are the most detailed spatially resolved temperature/soot statistics available from a fully turbulent fire plume of meaningful size and will be useful for the development and validation of new fire fluid dynamics codes.

Acknowledgements

The authors are grateful to Sheldon Tieszen of Sandia for many stimulating conversations regarding the physics of fire plumes and for his stalwart support of this project. This work is supported by Sandia National Laboratories and the United States Department of Energy. Sandia National Laboratories is a multi-program laboratory managed and operated by Sandia Corporation, a wholly owned subsidiary of Lockheed-Martin Company, for the U.S. Department of Energy's National Nuclear Security Administration under contract DE-AC04-94AL85000.

References

1. A. C. Eckbreth, *Laser Diagnostics for Combustion Temperature and Species*. Gordon and Breach: 1996.
2. S. R. Tieszen; T. J. O'Hern; E. J. Weckman; R. W. Schefer, *Combustion and Flame* **2004,** 139, 126-141.
3. T. J. O'Hern; E. J. Weckman; A. L. Gerhart; S. R. Tieszen; R. W. Schefer, *Journal of Fluid Mechanics* **2005,** 544, 143-171.
4. S. P. Kearney, in: *ASME International Mechanical Engineering Congress and Exposition (IMECE)*, New York, NY, 2001.
5. J. M. Suo-Anttila; T. K. Blanchat; A. J. Ricks; A. L. Brown, *Proceedings of the Combustion Institute* **2009,** 32, 2567-2574.
6. L. A. Gritzo; Y. R. Sivathanu; W. Gill, *Combustion Science and Technology* **1998,** 139, 113-136.
7. J. J. Murphy; C. R. Shaddix, *Combustion Science and Technology* **2006,** 178, 865-894.
8. S. P. Kearney; K. Frederickson; T. W. Grasser, *Proceedings of the Combustion Institute* **2009,** 32, 871-878.
9. K. Frederickson; S. P. Kearney; A. Luketa; J. C. Hewson; T. W. Grasser, *Combustion Science and Technology* **2010,** 182, 941-959.
10. K. Frederickson; S. P. Kearney; T. W. Grasser, *Applied Optics* **2011,** 50, (4), A49-A59.
11. T. K. Blanchat; T. J. O'Hern; S. P. Kearney; A. Ricks; D. Jernigan, *Proceedings of the Combustion Institute* **2009,** 32, (2), 2511-2518.
12. R. D. Hancock; F. R. Schauer; R. P. Lucht; R. L. Farrow, *Applied Optics* **1997,** 36, (15), 3217-3226.
13. R. J. Santoro; C. R. Shaddix, in: *Applied Combustion Diagnostics*, K. K. Hoinghaus; J. B. Jeffries, (Eds.) Taylor and Francis: 2002; pp 252-286.
14. A. C. Eckbreth; R. J. Hall, *Combustion and Flame* **1979,** 36, 87-98.
15. P. E. Bengtsson; M. Alden, *Combustion and Flame* **1990,** 80, 322-328.
16. S. P. Kearney; M. N. Jackson, *AIAA Journal* **2007,** 45, (12), 2947-2956.
17. T. Ni; J. A. Pinson; S. Gupta; R. J. Santoro, *Applied Optics* **1995,** 34, (30), 7083-7091.
18. R. E. Palmer *The CARSFT Computer Code for Calculating Coherent Anti-Stokes Raman Spectra: User and Programmer Information*; SAND89-8206; Sandia National Laboratories: Livermore, CA, 1989.
19. R. J. Santoro; H. G. Semerjian; R. A. Dobbins, *Combustion and Flame* **1983,** 51, 203-218.
20. J. Y. Zhu; D. Dunn-Rankin, *Applied Physics B* **1993,** 56, 47-55.
21. L. A. Gritzo; W. Gill; V. F. Nicolette *Estimates of the Extent and Character of the Oxygen-Starved Interior in Large Pool Fires, SAND97-2055J*; Sandia National Laboratories: Albuqueque, NM and Livermore, CA, 1997.
22. T. L. Henriksen; G. J. Nathan; Z. T. Alwahabi; N. Qamar; T. A. Ring; E. G. Eddings, *Combustion and Flame* **2009,** 156, 1480-1492.
23. Y. Xin; J. P. Gore, *Proceedings of the Combustion Institute* **2005,** 30, 719-726.

Figure Captions

Figure 1 – Digital photograph of the FLAME test-bay interior showing the position of the vertical lifting platforms, optical probes and horizontally movable fuel pan.

Figure 2 – Shot-averaged CARS spectrum from the center of the fire plume within the fuel-rich "vapor dome" region at y = 0.5 m (a). Single-laser-shot N_2 CARS spectra from the vapor dome region (b,c) and single-shot spectrum at y = 0.5 m above the fuel surface and x = 60 cm from the center of the fire plume.

Figure 3 – Representative single-laser-shot soot LII images from the 10% toluene in methanol pool fire.

Figure 4 – Mean and rms temperature and soot profiles at three heights above the liquid fuel surface.

Figure 5 – Temperature probability density function (pdf) evolution across the turbulent pool fire.

Figure 6 – Soot probability density function (pdf) evolution across the turbulent pool fire.

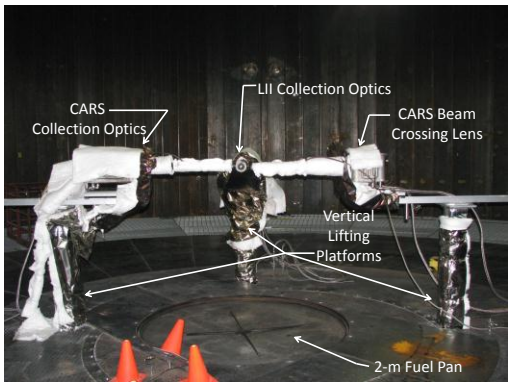
CARS
Collection Optics
LII Collection Optics
CARS Beam
Crossing Lens
Vertical
Lifting
Platforms
2-m Fuel Pan

Figure 1

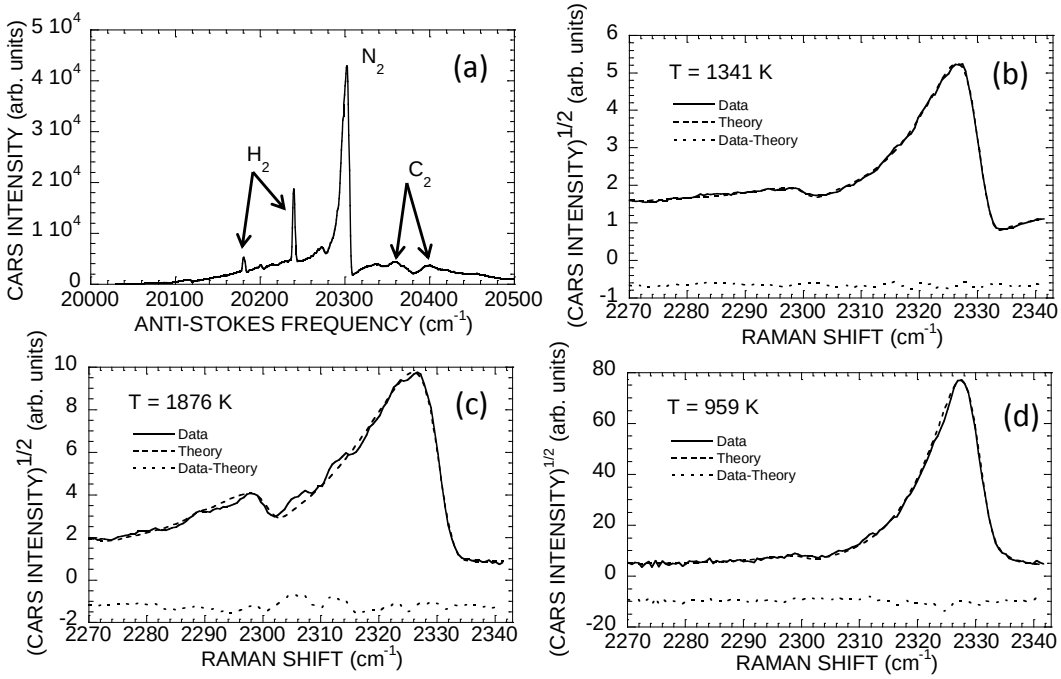
(a)
N2
H2
C2
CARS INTENSITY (arb. units)
ANTI-STOKES FREQUENCY (cm-1)
(b)
T = 1341 K
Data
Theory
Data-Theory
(CARS INTENSITY)1/2 (arb. units)
RAMAN SHIFT (cm-1)
(c)
T = 1876 K
(d)
T = 959 K

Figure 2

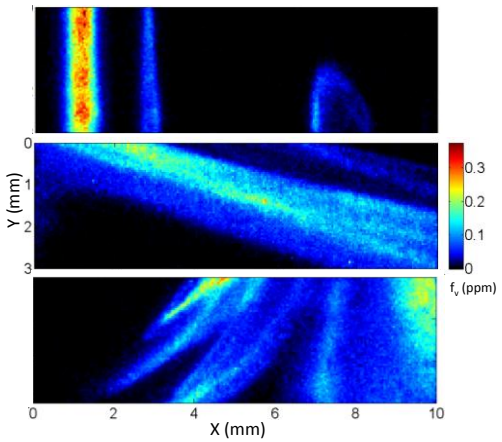

Figure 3

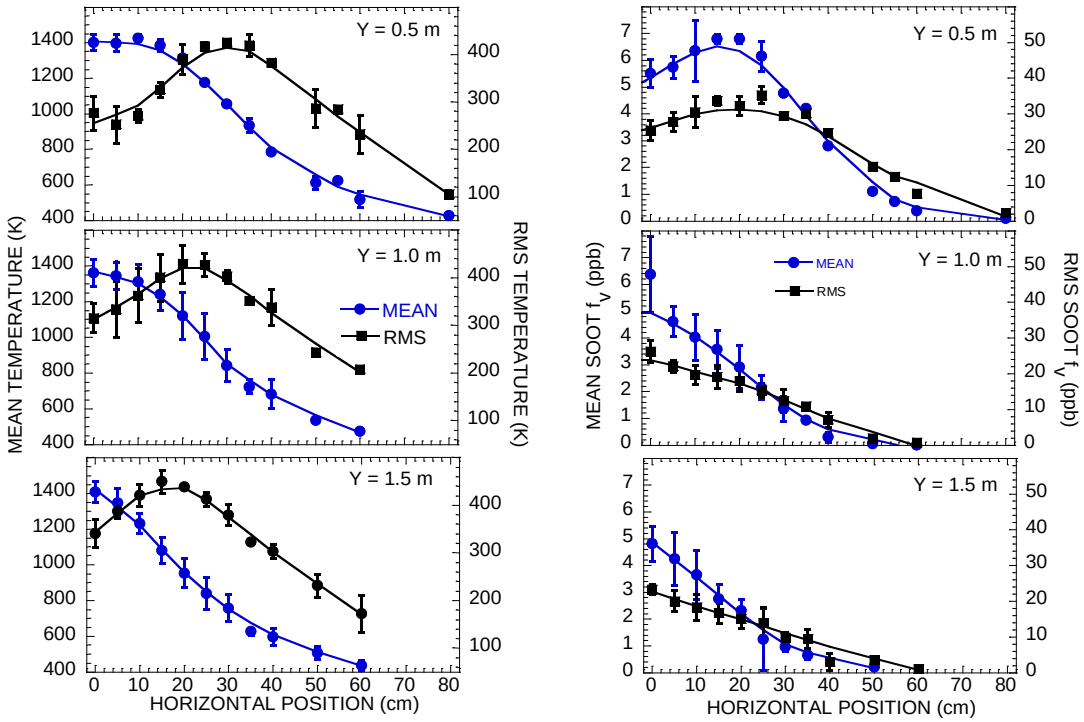
Y = 0.5 m
Y = 1.0 m
Y = 1.5 m
MEAN
RMS
MEAN TEMPERATURE (K)
RMS TEMPERATURE (K)
MEAN SOOT f_v (ppb)
RMS SOOT f_v (ppb)
HORIZONTAL POSITION (cm)

Figure 4

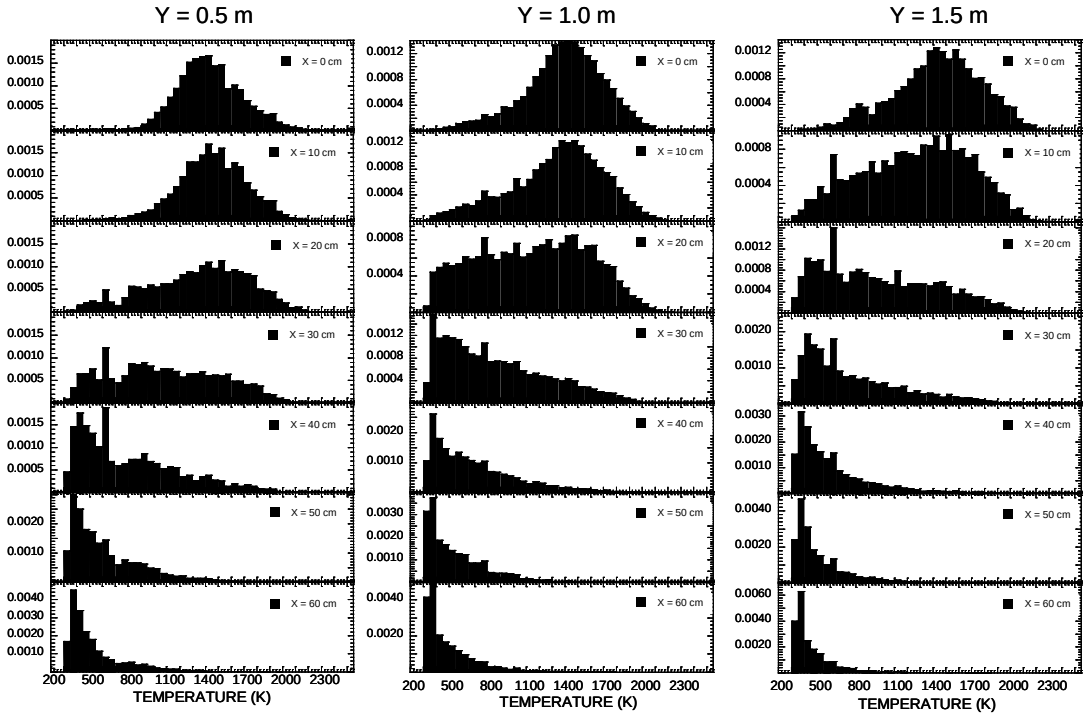
Y = 0.5 m
Y = 1.0 m
Y = 1.5 m
X = 0 cm
X = 10 cm
X = 20 cm
X = 30 cm
X = 40 cm
X = 50 cm
X = 60 cm
TEMPERATURE (K)
200 500 800 1100 1400 1700 2000 2300

Figure 5

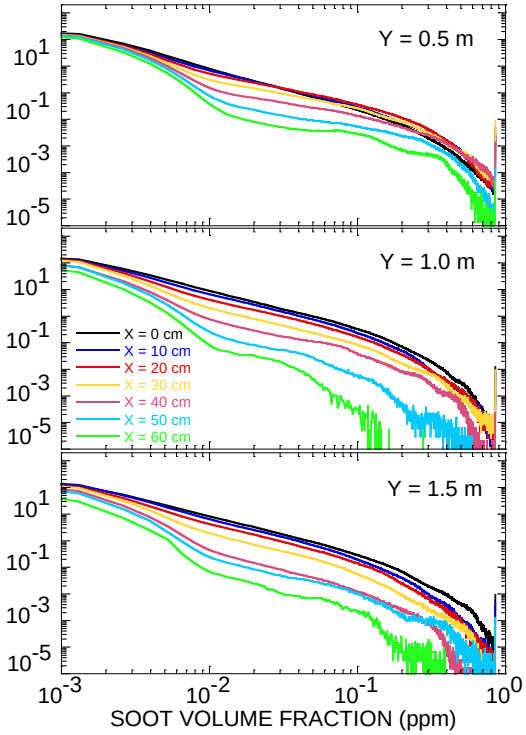
Y = 0.5 m
Y = 1.0 m
Y = 1.5 m
X = 0 cm
X = 10 cm
X = 20 cm
X = 30 cm
X = 40 cm
X = 50 cm
X = 60 cm
SOOT VOLUME FRACTION (ppm)

Figure 6